Altered Peripheral and Central Inflammatory Responses in a Mouse Model of Autism

Luciana Lucchina and Amaicha Mara Depino

Increasing clinical and experimental evidence links immune and inflammatory alterations with the pathogenesis of autism spectrum disorders (ASD). Autistic individuals show signs of neuroinflammation, altered inflammatory responses, and immune abnormalities throughout life. Mice injected subcutaneously with 600 mg/kg valproic acid (VPA600) at gestational day 12.5 show reduced social interaction in adulthood (at 8 weeks of age), and they have been proposed as a mouse model of autism. Here, we show that these adult animals present signs of chronic glial activation in the hippocampus and the cerebellum. Moreover, when they are challenged with a peripheral inflammatory stimulus (intraperitoneal lipopolysaccharides, LPS), VPA600 animals show an exacerbated inflammatory response. Two hours after LPS injection, VPA600 animals secrete more corticosterone to the blood than control mice, and show an increase in the levels of expression of proinflammatory cytokines in the spleen. After LPS challenge, VPA600 mice also show signs of increased neuroinflammation compared with control mice: they have more microglial cells in the hippocampus, and they show higher levels of proinflammatory cytokines in the cerebellum. Our results provide evidence of basal neuroinflammation and an altered inflammatory response in the VPA model of autism. We propose that this model can be used to evaluate the contribution of inflammatory reactivity to autism-related behaviors. These studies will contribute to elucidate the role of the inflammatory alterations observed in ASD individuals. ***Autism Res*** *2014, 7: 273–289.* © 2013 International Society for Autism Research, Wiley Periodicals, Inc.

Keywords: valproic acid; cytokines; microglia; astroglia; hypothalamus–pituitary–adrenal axis; behavior

Introduction

Autism spectrum disorders (ASD) are characterized by an impairment in social interactions, communication deficits, and restricted repetitive and stereotyped interests and behaviors [American Psychiatric Association, 2000]. The number of individuals diagnosed with ASD has increased in recent years, and it is reported to be as high as 9 per 1000 newborns [Centers for Disease Control and Prevention, 2009; Rutter, 2005]. Due to this increase in the prevalence of ASD and the general aging of society, it can be expected that the number of adult individuals with ASD will increase significantly in the next 20 years. However, most clinical and experimental studies have focused on the early processes that contribute to ASD symptoms, and only few reports are aimed at understanding the biological life-lasting alterations in ASD, and how they contribute to the pathophysiology of autism.

Both peripheral and brain inflammation have been associated with autism [reviewed in Depino, 2013; Onore, Careaga, & Ashwood, 2012; Patterson, 2011]. These immune alterations are not restricted to the perinatal period, but they seem to persist throughout life. Peripheral blood mononuclear cells and lymphoblasts from autistic children secrete more proinflammatory cytokines (particularly IL-1β, IL-6, and TNF-α) both basally [Malik et al., 2011] and after stimulation with bacterial endotoxin component lipopolysaccharides (LPS) [Jyonouchi, Sun, & Le, 2001] when compared with controls. Moreover, postmortem studies have shown that ASD subjects present neuroinflammation in various regions of the brain [Vargas, Nascimbene, Krishnan, Zimmerman, & Pardo, 2005], and that the neocortical transcriptome of autistic individuals reflects a strong immune response [Garbett et al., 2008]. However, the causes and consequences of these immune alterations have not been extensively explored.

Cytokines modulate normal neuronal function and behavior [Yirmiya & Goshen, 2011], and the bidirectional communication between the immune system and the brain is essential for the appropriate physiological and behavioral responses to infection [McCusker & Kelley, 2013]. However, chronic peripheral inflammation and abnormal inflammatory responses in the brain can lead to cognitive dysfunction, prolonged sickness behavior, and depression-like behavior. We can then hypothesize

From the Institute for Physiology, Molecular Biology and Neurosciences, CONICET-UBA, and Department of Physiology, Molecular and Cellular Biology, FCEyN, University of Buenos Aires, Buenos Aires, Argentina

Received March 19, 2013; accepted for publication September 3, 2013

Address for correspondence and reprints: Amaicha Mara Depino, Institute for Physiology, Molecular Biology and Neurosciences, CONICET-UBA. Int. Guiraldes S/N, Ciudad Universitaria, Pabellon 2, 2do piso, C1428EHA, Buenos Aires, Argentina. E-mail: adepino@conicet.gov.ar

Published online 3 October 2013 in Wiley Online Library (wileyonlinelibrary.com)
DOI: 10.1002/aur.1338

that altered inflammatory function and chronic glial activation in ASD could at least in part be responsible for the characteristic alterations in behavior observed.

ASD individuals are prone to suffer from chronic gastrointestinal disturbances [Hornig et al., 2008; Parracho, Bingham, Gibson, & McCartney, 2005; Wang, Tancredi, & Thomas, 2011], and these and other long-lasting inflammatory processes could underlie the immune alterations observed in ASD. Alternatively, autistic individuals can have an abnormal immune system, which would in turn make them more prone to chronic infection and autoimmune disorders. Recent studies in mice have shown indeed that maternal immune activation can alter the behavior of the offspring, resulting in reduced sociability and other behaviors related to autism [Malkova, Yu, Hsiao, Moore, & Patterson, 2012]. Moreover, these animals also show immune dysregulation [Hsiao, McBride, Chow, Mazmanian, & Patterson, 2012]. This goes in line with the clinical evidence linking perinatal infection with autism [reviewed in Depino, 2013]. However, other proposed genetic and environmental etiological factors could either affect immune function or make the subjects more susceptible to infection and disease.

Our aim here was to characterize the peripheral and central inflammatory responses in a non-inflammatory model of autism. To this aim, we chose to study the valproic acid (VPA) model of autism in mice. Clinical evidence associated the prenatal exposure to the antiepileptic drug VPA to a high incidence of autism [Moore et al., 2000]. Following that evidence, different studies have shown that prenatal exposure to 600 mg/kg VPA at the gestational day (GD) 12.5 results in reduced sociability in the rat [Kim et al., 2011; Schneider & Przewlocki, 2005] and in the mouse [Wagner, Reuhl, Cheh, McRae, & Halladay, 2006]. Similarly, children prenatally exposed to VPA showed poor social interaction and communication skills [Moore et al., 2000]. Therefore, this pharmacological treatment is considered to be an animal model of autism, showing construct and face validity.

Here, we used this mouse model to characterize the basal inflammatory state and the response to an acute inflammatory stimulus, both in the periphery and in the brain. We show that animals prenatally exposed to VPA show reduced social interaction and increased anxiety-related behavior in the elevated plus maze (EPM). Moreover, they present evidence of long-lasting glial activation in the hippocampus and the cerebellum, and they respond in an exacerbated way to an inflammatory stimulus.

Methods

Animals

BALB/cAnNCr1 (BALB/c, Charles River, Wilmington, MA, USA) and C57BL/6J (C57, The Jackson Laboratory, Bar Harbor, Maine, USA) strains were bred for several generations in the animal house at the Leloir Institute (Buenos Aires, Argentina). To obtain F1 hybrid offspring, BALB/c females were mated with C57 males at 8–12 weeks of age. Analysis of F1 hybrid mice has been advised due to the facts that they are genetically and phenotypically uniform, and that they possess hybrid vigor [Banbury Conference, 1997]. Each male mouse was bred with one nulliparous female. Female mice were controlled daily and placed in a single cage when a vaginal plug was observed. This day was considered GD0.5. At GD12.5, pregnant mice were injected subcutaneously with 400 or 600 mg/kg of valproic acid sodium salt in saline solution (VPA; Sigma, St. Louis, MO, USA). Control animals were injected with saline solution (CON). The day of parturition was defined as postnatal day (PD) 0. The litters were culled to 10 pups and weaned at PD21 in cages containing four to six animals. Only the male mice were studied. Offspring belonging to the same treatment group were mixed at weaning to reduce the litter effect. Two independent cohorts were used, with a total of 5–6 litters per each prenatal treatment. For each experimental group, 20 mice were studied. To reduce the number of animals used, the response to an inflammatory stimulus was studied in the same groups of animals that were subjected to behavioral analysis.

All animals had water and food *ad libitum* and were housed on a 12:12 light/dark cycle with lights on at 8:00 am. All animal procedures were performed according to the regulations for the use of laboratory animals of the National Institute of Health, Washington, DC, USA (followed by the Leloir Institute).

Behavioral Testing

Behavioral testing was performed during the light period (between 10:00 and 16:00 hr) under dim light illumination. Mice were 8–10 weeks of age at the beginning of testing. Tests were separated by 1-week intervals to reduce inter-test interactions and performed in the order listed below. Mice were tested in the holding room. After changing illumination, mice were habituated to it for 45 min prior to the test. After testing, each mouse was identified and placed in a holding cage until all animals in a cage were tested. Each apparatus was cleaned with 20% ethanol between sessions. All testing and manual scoring was performed by an experimenter (L.L.) blinded to treatment groups.

The social interaction test was performed as previously described [Depino, Lucchina, & Pitossi, 2011]. Briefly, a 40×15 cm black arena divided in three compartments (side compartments: 15×15 cm, central compartment: 10×15 cm) was used. Openings that measure 7.5 cm connected the central and side compartments. A clear Plexiglass cylinder (7.5 cm of diameter, with several holes to allow nose contact) was placed in each side compart-

ment at the beginning of the test. Animals were placed in the central compartment and allowed to explore for 5 min (habituation). Then, an unfamiliar, young (3 weeks of age) C57 male mouse (social stimulus) was placed in one of the cylinders. Social interaction was evaluated during a 10 min period. The social side was randomly chosen. The amount of time spent in each compartment and locomotion data were collected by a video-tracking system (ANY-maze, Stoelting, IL, USA). The time the subject spent sniffing the social stimulus (nose inside a hole of the cylinder) was recorded manually using a key.

The EPM was performed as previously described [Depino et al., 2011; Depino, Tsetsenis, & Gross, 2008; Lucchina, Carola, Pitossi, & Depino, 2010]. The maze consisted of two open and two closed arms (open arms: 30 × 5 cm, 105 lux, surrounded by a 0.5 cm high border; closed arms: 30 × 5 cm, 43 lux, surrounded by 19 cm high walls). The walls were made of black polyvinyl chloride (PVC) and the floor of gray PVC. The apparatus was elevated 50 cm above the floor. Mice were placed into the central platform (5 × 5 cm, 102 lux) of the maze facing toward an open arm and allowed to explore the maze for 5 min. Locomotion data were collected by the ANY-maze system (Stoelting), and rearing events were scored manually during each session. We measured two parameters of exploration (total distance walked and the number of rearing events) and two anxiety-related variables (time spent in the open arms and percentage of distance in the open arms).

The open field (OF) test was performed as previously described [Depino et al., 2008, 2011; Lucchina et al., 2010]. Mice were placed in an arena (floor: 45 × 45 cm of gray PVC; walls: 30 cm high of black formic; 30 lux) for 5 min. Animals were initially placed along one side of the arena, and the center region was defined as the central 23 × 23 cm area. Locomotion data were collected by the ANY-maze system (Stoelting), and rearing events were scored manually during each session. We analyzed two exploratory variables (total distance walked and the number of rearing events) and two anxiety-related parameters (time spent in the center and percentage of distance in the center).

The novel object recognition test was performed as previously described [Depino et al., 2008, 2011]. Time exploring each object was measured during each session (orientation of the animal toward the object with its nose within 1 cm of the object for a minimum of 1 sec), using the ANY-maze software (Stoelting).

The tail suspension test was performed as previously described [Depino et al., 2011]. Animals were suspended in the air using adhesive tape wrapped around the subject's tail (about 4/5 from the base) and fixed to a wire at 25 cm of height from a wooden surface. The time spent immobile was measured during 5 min. Animals that learned how to climb their own tails during the test were removed from the analysis.

The forced swimming test was performed as previously described [Depino et al., 2011]. Subjects were gently placed in a beaker glass (diameter, 15 cm; height, 25 cm), filled with 14 cm of water at room temperature (25°C). The time spent immobile during 5 min was measured with a stopwatch. At the end of the test, animals were dried with a paper towel, and they were placed in a holding cage with normal bedding. Mice were dry after 20 min.

Adult LPS Challenge

One week after the last behavioral test, animals from each prenatal treatment were randomly assigned to two experimental groups: LPS or saline (adult treatment). Animals were injected intraperitoneally either with 25 µg/kg LPS (*Escherichia coli* LPS, serotype 0111:B4, Sigma) or with sterile saline solution (Sal). Two hours after the injection, animals were deeply anesthetized and sacrificed. We chose this time as it was previously shown to be the peak of blood corticosterone levels after LPS injection [Pitossi, del Rey, Kabiersch, & Besedovsky, 1997]. All LPS and saline injections occurred between 9:00 and 10:00 am to avoid the effect of corticosterone circadian variations. For corticosterone and cytokines analysis, trunk blood was collected from the heart, and then the spleen and brain tissues (hippocampus and cerebellum) were dissected and snap-frozen in liquid nitrogen. For immunohistochemical analysis, animals were perfused as it is described below. To evaluate whether VPA can activate the hypothalamus–pituitary–adrenal (HPA) axis, we injected 600 mg/kg VPA or saline solution, we collected trunk blood 2 hr after injection, and we performed radioimmunoassay (RIA) as described.

Corticosterone RIA

RIA was performed on plasma samples as previously described [Lucchina et al., 2010]. Trunk blood samples were centrifuged, and the plasma was removed and stored at –20°C until RIA was performed. Corticosterone was extracted twice from plasma, using 500 µL and 300 µL of ether, respectively, and resuspended in 100 µL of buffer B (0.05 M Tris pH 8, 0.1 M NaCl, 0.1% sodium azide and 0.1% BSA). The assay was carried out following the RIA protocol provided by the anti-corticosterone antibody manufacturer (C8784, Sigma) using ^{3}H-corticosterone (1,2,6,7-^{3}H(N)-corticosterone, Perkin-Elmer, Waltham, MA, USA). The lower limit of detection of the assay was 12.5 pg corticosterone.

Real-Time RT-PCR

RNA isolation and reverse transcription were performed as previously described [Depino, Ferrari, Pott Godoy, Tarelli,

& Pitossi, 2005]. Comparative quantitation by real-time RT-PCR was performed for each cytokine using the SYBR-green I fluorescence method, with Rox as passive reference dye [Depino et al., 2011]. Stratagene MxPro TM QPCR software and Stratagene Mx3005P equipment were used (Agilent Technologies, Santa Clara, CA, USA).

Primers and product size are presented in Table 1. A standard curve was performed for each molecule alongside with the samples, and used to transform Ct values to cDNA dilution values. cDNA levels of cytokines were then normalized with the cDNA level of β2-microglobulin in the same sample. We used β2-microglobulin as house-keeping gene because its expression was not altered by the treatments (data not shown). Results were confirmed by normalization with β-actin, with the exception of the hippocampus, where this house-keeping gene showed effects of both prenatal and adult treatments (data not shown). All samples were run in triplicate. Specificity was controlled by melting curves and electrophoresis in agarose gels. Values are expressed as percentage of the CON-Sal group.

Immunohistochemistry

Animals were deeply anesthetized and transcardially perfused with heparinized saline followed by cold 4% paraformaldehyde in 0.1 M phosphate buffer (pH = 7.2). After removing the brains, they were placed in the same fixative for 4–5 hr at 4°C. Then, the brains were cryoprotected by immersion in 30% sucrose, frozen in isopentane, and 40 µm-thick serial sections were obtained in a cryostat. The brains were sectioned in the coronal plane, whereas the cerebella were sectioned in the sagittal plane.

For immunohistochemical identification of microglial and astroglial cells, every 12th section (each 440 µm apart) was processed as previously described [Depino et al., 2011]. Briefly, free-floating sections were treated with 2% H_2O_2 in methanol for 10 min, and nonspecific protein binding was blocked by the incubation with 1% normal donkey serum in Tris-buffered saline (TBS) for 1 hr (containing 1% of triton for microglia and 0.1% for astroglia). Sections were incubated with primary antibodies rat anti-mouse CD11b (1:500, Serotec, Oxford, UK) or rabbit anti-glial fibrillary protein (GFAP) (1:700, DAKO, Glostrup, Denmark), overnight at room temperature. Anti-rat and anti-rabbit biotinylated secondary antibodies (Jackson Laboratories, West Grove, PA, USA) followed by Vectastain standard ABC kit (Vector Laboratories, Burlingame, CA, USA) were used. For each brain structure, three sections per animal were analyzed for each marker.

Stereological Analysis

Stereological quantifications were performed by an observer (L.L.) blinded to the treatment using a Nikon Eclipse E600 microscope and a CX900 video camera (MicroBrightField Inc., Williston, VT, USA), with the aid of the Stereo Investigator image analysis software (MicroBrightField Inc.). The optical fractionator method [West, Slomianka, & Gundersen, 1991] was employed to estimate the number of microglial cells in the cerebellum, and in the molecular layer, granular cell layer, and hilus of the dentate gyrus (DG) of the hippocampus. Zones were delineated with the tracing function of the Stereo Investigator software using a 10 × magnification objective (0.4 NA), according to a mouse brain atlas [Paxinos & Franklin, 2001]. A preliminary population estimate was performed to determine the desired parameters. We used a 50 × 50 × 10 µm counting frame and a 150 × 150 µm sampling grid to analyze the cerebellum, and a 70 × 70 × 9 µm counting frame and a 200 × 200 µm sampling grid for the various areas of the hippocampus. Guard zones were 2 µm. The CD11b-positive cells were counted using a 60X oil lens, following the unbiased sampling rule [Howard & Reed, 2005], and included in the measurement when they came into focus within the optical dissector. The cellular body size was measured with the Nucleator probe. Five isotropic rays were used to determine the soma volume. For the analysis, the number and volume of cells and the volume of the brain region were taken into account for each animal and averaged per group.

Estimation of GFAP-Positive Area

Sections were analyzed under an Olympus microscope (Center Valley, PA, USA), and digital images were obtained

Table 1. Primers Used in Real-Time RT-PCR Analyses and Expected Product Sizes

Molecule	5' primer	3' primer	Product size
IL-1β	TTGACGGACCCCAAAAGATG	AGAAGGTGCTCATGTCCTCA	204
IL-6	GTTCTCTGGGAAATCGTGGA	TGTACTCCAGGTAGCTATGG	208
TNF-α	TCTCATCAGTTCTATGGCCC	GGGAGTAGACAAGGTACAAC	212
TGF-β1	TGACGTCACTGGAGTTGTACGG	GGTTCATGTCATGGATGGTGC	170
β2m	TGACCGGCTTGTATGCTATC	CAGTGTGAGCCAGGATATAG	222

using a 10 × magnification lens, with an Infinity2 camera and the Infinity Capture software (Lumera Corporation, Ottawa, ON, Canada). The percentage of the area immunoreactive for GFAP was measured in digital images with the aid of the ImageJ software [Rasband, 1997–2009] as previously described [Depino et al., 2011]. Briefly, the threshold was manually set so that all immunostained cells were selected. Then, the percentage of the area occupied by astrocytes was measured in each region studied.

Stereotaxic Injections

Adult male mice were anesthetized with ketamine chlorhydrate (80 mg/kg) and xylazine (8 mg/kg). Ten micrograms of LPS in 1 µL were administered with a 50-µm tipped finely drawn glass capillary. Control mice received 1 µL of saline solution. The stereotaxic coordinates were as follows: bregma, –6.9 mm; ventral, –1 mm. For lobules VI–VII, we leveled the skull by aligning the tooth bar to the ear bars. For lobules IV–V, we adjusted the tooth bar 3 mm lower than the ear bars. Eight animals per group were injected.

Animals were kept in a cage placed over a heating pad until they woke up. Twenty-four hours after injection, mice were evaluated in the social interaction test and weighed. After testing, animals were perfused and their cerebella analyzed for glial activation as previously described. We verified the site of injection in each animal using Nissl-stained tissue and removed from the analysis those animals in which the corresponding lobule was not targeted.

Statistical Analysis

Statistical analysis was performed with the aid of the Statistica software (version 7, StatSoft Inc., Tulsa, OK, USA). One-way or two-way analysis of variance (ANOVA) was performed, followed by Tukey's multiple comparisons test. In all cases, statistical significance was assumed where $P < 0.05$. Data are presented as mean ± SEM.

Results

Prenatal Exposure to VPA Results in Autism-Related Behaviors

In order to characterize the effects of prenatal exposure to VPA on the inflammatory response, we first confirmed the behavioral phenotype of the model by comparing control mice (CON) with mice exposed to 600 mg/kg VPA (VPA600, a dose previously shown to result in reduced social interaction) and with mice exposed to a lower dose of 400 mg/kg (VPA400). We observed no effect of VPA treatment on the length of gestation or on the number of pups per litter (data not shown). Moreover, unpublished data from our lab shows that VPA does not alter maternal behavior, and we found that all mice gained weight similarly during the first postnatal week [weight at PD7, CON 3.87 ± 0.19 g, VPA400 4.30 ± 0.15 g, VPA600 3.93 ± 0.11 g; ANOVA $F(2, 57) = 2.269$, $P = 0.113$]. In summary, we found no strong effect of VPA on mice development.

When mice reached adulthood (at the eighth postnatal week), we started the behavioral analysis.

Social interaction deficits. All animals showed the same levels of total locomotion in the social interaction test (SI), both in the habituation stage [$F(2, 44) = 2.498$, $P = 0.094$] and in the social interaction stage [$F(2, 44) = 2.011$, $P = 0.146$; Fig. 1A]. Although all animals showed preference for the social compartment during the social interaction stage (Fig. 1B), we observed a significant effect of prenatal treatment with VPA on the time that animals spent interacting with the stimulus mouse [$F(2, 44) = 5.447$, $P = 0.008$], with VPA600 animals spending less time sniffing the stimulus than CON mice (Fig. 1C). This effect was not due to a general neophobic response, as VPA600 and CON mice responded in a similar manner to a novel object in the novel object recognition test [time exploring the novel object, CON 136.2 ± 9.5 sec, VPA600 126.9 ± 13.3 sec, $t(30) = 0.554$, $P = 0.583$]. A lower VPA dose (400 mg/kg) showed an intermediate response in the time spent sniffing the stimulus mouse (Fig. 1C).

Anxiety-related behavior. As mood disorders and anxiety disorders show a high comorbidity with ASD [American Psychiatric Association, 2000; Hofvander et al., 2009], we also studied anxiety- and depression-related behaviors in mice exposed to VPA. To assess anxiety-related behavior, we performed the EPM and the OF tests. For the EPM, ANOVA showed that VPA400 and VPA600 offspring walked less [$F(2, 50) = 5.565$, $P = 0.007$; Fig. 1D]. Moreover, VPA600 showed less vertical explorations [CON 11.50 ± 1.02, VPA400 13.78 ± 1.16, VPA600 8.88 ± 1.25; $F(2, 50) = 4.536$, $P = 0.016$]. VPA600 mice spent less time in the open arms [$F(2, 50) = 4.551$, $P = 0.015$; Fig. 1E] and showed a reduced percentage of distance walked in the open arms [$F(2, 50) = 5.066$, $P = 0.010$; Fig. 1F].

For the OF, ANOVA showed no differences between groups in the total distance walked, the time spent in the center, or the percentage of distance walked in the center. Only a significant effect on the number of vertical explorations was observed, with VPA400 and VPA600 showing a significantly reduced number of events [CON 33.26 ± 1.95, VPA400 25.37 ± 1.92, VPA600 24.44 ± 1.55; $F(2, 53) = 7.107$, $P = 0.002$]. In summary, VPA600 mice showed an increased anxiety-related phenotype in the EPM, but not in the OF.

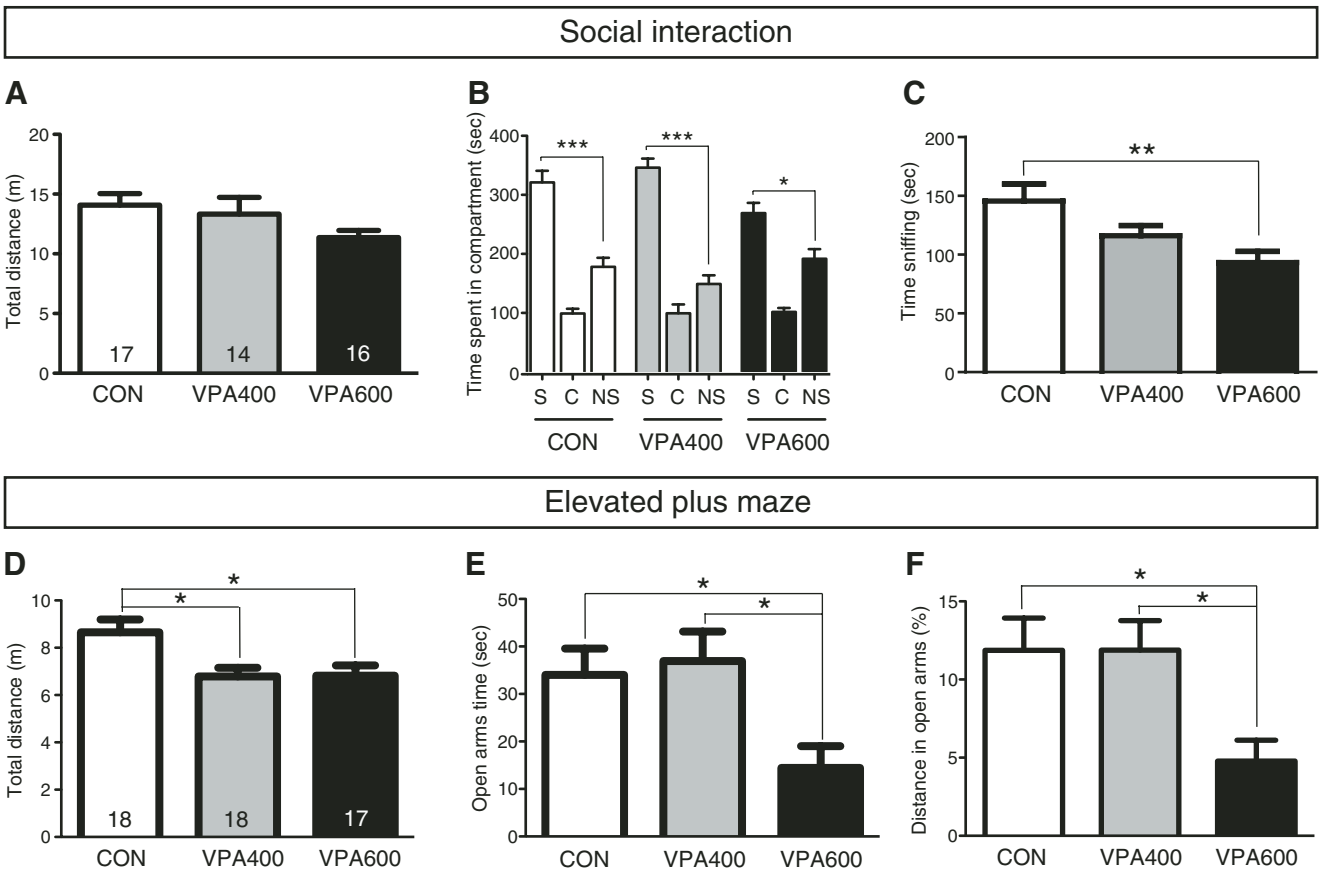

Figure 1. Prenatal exposure to valproic acid (VPA) results in increased autism- and anxiety-related behaviors in adult mice. In the social interaction test, animals show similar levels of exploration during the social interaction test (A) and preference for the social compartment (B), but they spend less time sniffing the social stimulus (C). VPA-exposed mice also show increased anxiety-related behavior in the elevated plus maze (EPM): VPA 400 and VPA600 animals explore less the EPM (D), and VPA600 mice spend less time (E) and walk less (F) in the open arms. $*P < 0.05$, $**P < 0.01$, $***P < 0.001$, Tukey's multiple comparison test. Mean ± SEM. Ns are shown in each bar. S, social compartment; C, central compartment; NS, non-social compartment.

Depression-related behavior. We evaluated immobility in the forced swimming and tail suspension tests, a variable that is affected by rodent treatment with antidepressant drugs and which has been interpreted as "behavioral despair." VPA600 mice spent the same amount of time immobile in these tests when compared with CON mice [forced swimming test, CON 231.5 ± 5.5 sec, VPA600 231.1 ± 3.2 sec, $t(31) = 0.064$, $P = 0.949$; tail suspension, CON 90.6 ± 8.3 sec, VPA600 116.4 ± 16.5 sec, Welch-corrected $t(23) = 1.398$, $P = 0.175$).

Mice Prenatally Exposed to VPA Show an Exacerbated Peripheral Inflammatory Response to LPS

To examine whether the prenatal exposure to VPA could induce changes in the peripheral inflammatory response, we injected LPS or saline intraperitoneally in adult animals (adult treatment) and we evaluated the inflammatory response 2 hr later. Intraperitoneal injection of LPS has been extensively used to mimic bacterial infection, and has been widely used to study acute inflammatory responses in the periphery and in the brain [Pitossi et al., 1997]. In particular, we measured plasma corticosterone levels and the expression of cytokines in the spleen (a classical peripheral site of cytokine production).

Two-way ANOVAs were performed with prenatal treatment (three levels: CON, VPA400, and VPA600) and adult treatment (two levels: Sal and LPS) as independent variables. We observed an interaction between prenatal and adult treatments in the levels of plasma corticosterone [$F(2, 20) = 5.874$, $P = 0.009$]. For Sal animals, there were no differences in the levels of corticosterone between VPA-exposed and CON adult offspring. The injection of LPS activated the HPA axis in all animals, but this response was exacerbated in VPA600 mice (Fig. 2A).

As it has been shown that prenatal inflammatory stimuli can result in long-lasting alterations in behaviors related to ASD [Malkova et al., 2012], that and early life

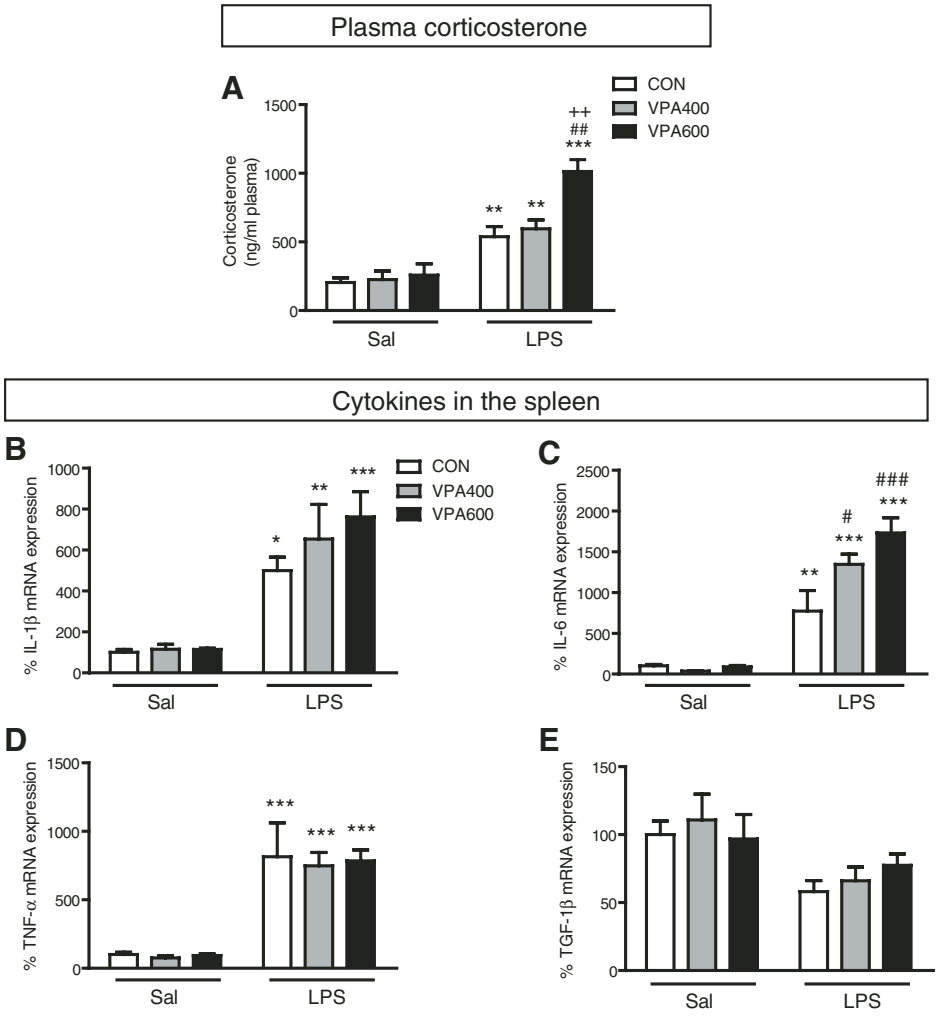

Figure 2. Mice prenatally exposed to valproic acid (VPA) show increased peripheral responses to an inflammatory stimulus. (A) Lipopolysaccharide (LPS) activates the hypothalamus–pituitary–adrenal axis, but the amount of plasma corticosterone is higher in VPA600 mice. $N = 4–5$ per group. In the spleen, LPS increases the expression of proinflammatory cytokines and reduces the expression of the anti-inflammatory cytokine TGF-β1. All animals show increased levels of IL-1β (B), IL-6 (C), and TNF-α (D) upon LPS challenge. The increase of IL-6 was exacerbated in VPA-exposed mice. There was a general reduction in the levels of TGF-β1 after LPS challenge (E). $N = 4–6$ per group. Tukey's multiple comparison test: $*P < 0.05$, $**P < 0.01$, $***P < 0.001$ vs. the corresponding Sal group; $\#P < 0.05$, $\#\#P < 0.01$, $\#\#\#P < 0.001$ vs. CON-LPS group; $++P < 0.01$ vs. VPA400-LPS group. Mean ± SEM.

inflammation can also result in altered HPA function [Shanks et al., 2000], we asked whether VPA could actually elicit an inflammatory response in mice. To test for this, we injected adult mice with 600 mg/kg of VPA or saline solution, and collected trunk blood 2 hr after injection. We found no effect of VPA on the levels of plasma corticosterone [Saline 64.2 ± 13.2 ng/mL, VPA 83.7 ± 41.7 ng/mL; $t(6) = 0.55$, $P = 0.60$].

LPS elicited the expression of IL-1β, IL-6, and TNF-α in the spleen of all animals [adult treatment effect: IL-1β, $F(1, 24) = 52.263$, $P < 0.001$; IL-6, $F(1, 24) = 145.781$, $P < 0.001$; TNF-α, $F(1, 24) = 79.046$, $P < 0.001$; Fig. 2B–D] and reduced the expression of TGF-β1 [$F(1, 24) = 10.600$, $P = 0.003$; Fig. 2E]. In addition, IL-6 also showed an effect of prenatal treatment [$F(2, 24) = 7.434$, $P = 0.003$] and an interaction between treatments [$F(2, 24) = 8.008$, $P = 0.002$]. VPA400 and VPA600 mice challenged with LPS showed higher IL-6 mRNA levels in the spleen than CON mice after the inflammatory stimulus (Fig. 2C).

Mice Prenatally Exposed to VPA Show Signs of Glial Activation and Exacerbated Central Inflammatory Responses to a Peripheral LPS Challenge

We analyzed the effect of prenatal VPA exposure and adult LPS challenge on the extent of astroglial and microglial activation in two brain regions linked to autism-related behaviors in the mouse (namely, social

interaction and repetitive behaviors): the hippocampus [Depino et al., 2011] and the cerebellum [DeLorey, Sahbaie, Hashemi, Homanics, & Clark, 2008; Martin, Goldowitz, & Mittleman, 2010]. In a preliminary study, we evaluated which area within each structure to quantify, considering whether qualitative differences were observed and if the structure showed a homogeneous pattern of glial cells or if it was more appropriate to create subdivisions. In all cases, two-way ANOVA (prenatal × adult treatments) and Tukey's post-hoc tests are reported.

Hippocampus. Three different subareas of the DG of the hippocampus were analyzed: the molecular layer, the granular cell layer, and the hilus. In the molecular layer, stereological quantification of microglia showed effects of both prenatal treatment [$F(2, 15) = 4.032$, $P = 0.040$] and adult treatment [$F(1, 15) = 8.331$, $P = 0.011$] in a two-way ANOVA. The density of microglial cells in this region was higher in VPA600 than CON mice, when they had been challenged with LPS 2 hr earlier (Fig. 3A and Fig. S1A). The area occupied by astrocytes was also affected by the prenatal [$F(2, 18) = 4.689$, $P = 0.023$] and the adult treatments [$F(1, 18) = 10.889$, $P = 0.004$]. There was a general increase in the GFAP-positive area in animals challenged with LPS (Fig. 3E). In the granular cell layer of the DG, we observed an effect of adult treatment on the density of microglial cells [$F(1, 15) = 7.277$, $P = 0.017$]. VPA600 mice injected with LPS showed a tendency to increased number of microglial cells when compared with VPA600 animals injected with saline ($P = 0.051$; Fig. 3B). In this region, we observed the effects of both prenatal [$F(2, 18) = 3.599$, $P = 0.048$] and adult treatments [$F(1, 18) = 29.712$, $P < 0.001$] on the extension of the GFAP-positive area. In VPA400 and VPA600 mice, the LPS challenge increased the area occupied by astrocytes, something that was not observed in CON-LPS mice (Fig. 3F). In the hilus, the analysis of microglia showed effects of both prenatal [$F(2, 15) = 6.879$, $P = 0.008$] and adult treatments [$F(1, 15) = 7.720$, $P = 0.014$). Only VPA600 mice showed increased microglial cell density upon a peripheral LPS challenge (Fig. 3C). In this region, the area occupied by astrocytes was only affected by the adult treatment [$F(1, 18) = 21.337$, $P < 0.001$]. There was a general increase in the GFAP-positive area after LPS injection that reached statistical significance for the VPA400 group (Fig. 3G and Fig. S2A).

In the CA1 of the hippocampus, the density of microglial cells was affected by both the prenatal [$F(2, 15) = 22.135$, $P < 0.001$] and the adult treatments [$F(1, 15) = 18.650$, $P < 0.001$]. Prenatal exposure to 600 mg/kg VPA resulted in more microglial cells in this region, and the adult challenge with LPS further augmented the number of these cells in these animals (Fig. 3D and Fig. S1B). In the CA1, the percentage of GFAP-positive area showed an interaction between prenatal and adult treatments [$F(2, 18) = 7.407$, $P = 0.004$]. CON mice showed an increase in the GFAP-positive area after the injection of LPS in adulthood, but in VPA400 and VPA600 animals this effect was not observed (Fig. 3H and Fig. S2B).

When we analyzed the size of the soma of microglial cells present in the hippocampus, we observed that both the prenatal [$F(2, 15) = 12.308$, $P < 0.001$] and the adult treatments [$F(1, 15) = 45.456$, $P < 0.001$] affected this parameter. Prenatal exposure to 400 mg/kg VPA and adult LPS challenge increased the size of the microglial cell body (Fig. 3I), suggesting that these stimuli turn these cells to a more activated state.

Cerebellum. Microglial cells showed a homogeneous distribution through the molecular, granular, and pyramidal layers of the cerebellum, and they were mostly excluded from the white matter. For this reason, the white matter was not included for quantification, and the other layers were stereologically sampled for estimation of microglial cell number. We observed an interaction between prenatal and adult treatments [$F(2, 18) = 5.849$, $P = 0.011$] in the density of microglial cells in the cerebellum. VPA600-Sal mice showed higher density of microglial cells than CON-Sal animals (Fig. 4A and C). When animals were challenged with LPS, we detected a significant increase in the number of these cells in CON animals. However, after LPS, all animals showed similar densities of microglial cells, suggesting that the effects of prenatal and adult treatments were not additive, or that there is a ceiling effect that prevents further increases in VPA600 mice. However, the size of the soma was only affected by the adult treatment [$F(1, 18) = 27.676$, $P < 0.001$]. LPS significantly increased the size of the microglial cells soma in animals prenatally exposed to 600 mg/kg VPA, suggesting activation of these cells in this experimental group (Fig. 4B).

GFAP-positive cells show a very characteristic distribution in the cerebellum: the cell bodies of Bergmann's glial cells are allocated among the cell bodies of Purkinje cells, and they project their processes across the molecular layer. We, therefore, delimitated two areas: the molecular layer (including the cell bodies of Bergmann's glial cells) and the granular cell layer. In the molecular layer, a two-way ANOVA showed an effect of the adult treatment on the percentage of area occupied by astrocytes [$F(1, 17) = 7.815$, $P = 0.012$] due to a general decrease in this area in LPS-injected mice (Fig. 4D). VPA and LPS treatments did not affect the percentage of GFAP-positive area in the granular cell layer (Fig. 4E). We then studied whether the analysis of the whole cerebellum was obscuring alterations in the GFAP-positive area in specific

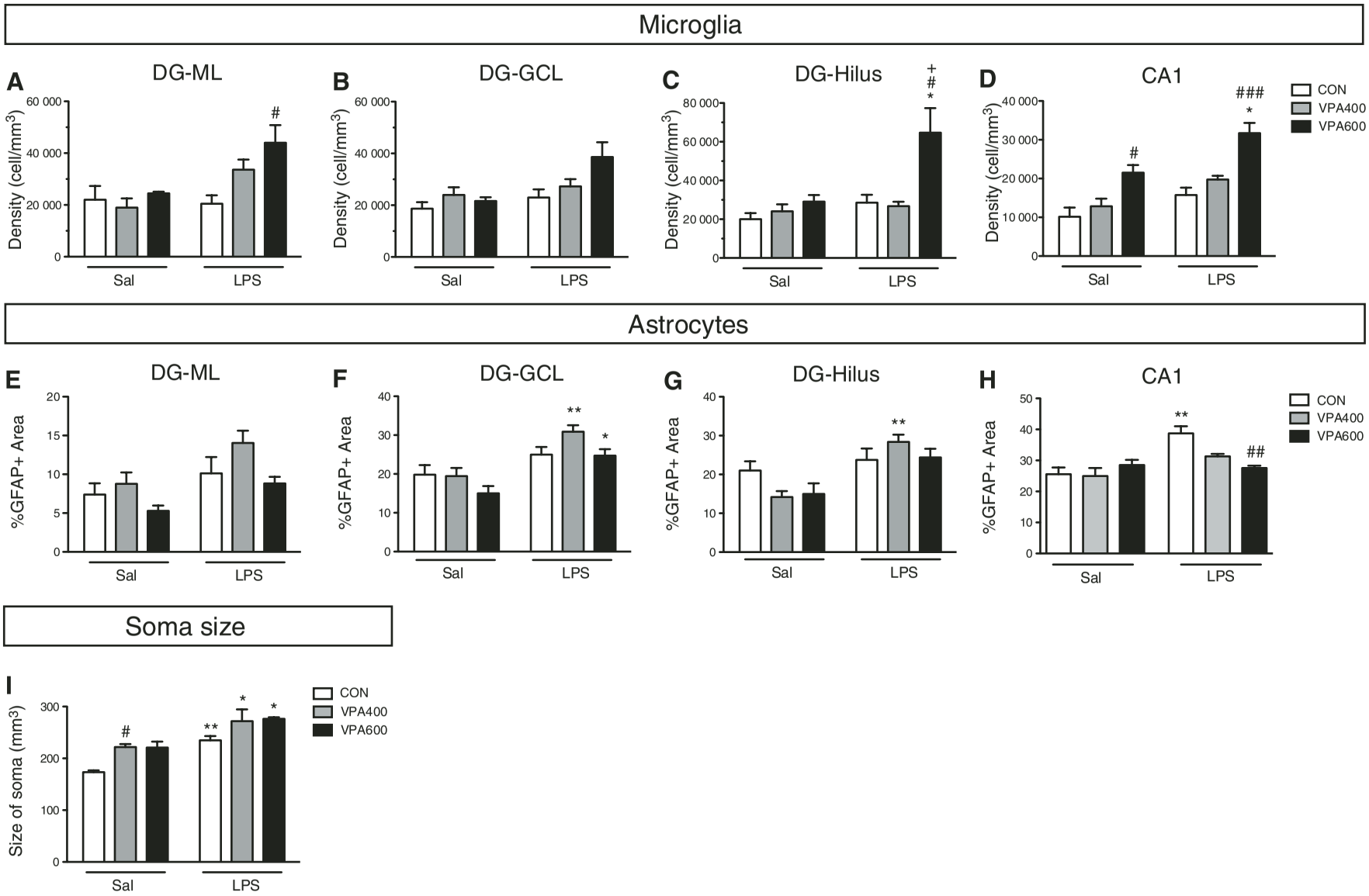

Figure 3. Mice prenatally exposed to valproic acid (VPA) show increased glial activation in the hippocampus. Stereological analysis of the number of microglial cells (CD11-positive) in the dentate gyrus (DG) (A–C) and the CA1 (D) of the hippocampus show that there is an increase in the number of these cells in animals prenatally exposed to VPA and challenged with lipopolysaccharides (LPS) in adulthood. LPS tends to increase the size of the soma of microglial cells in the hippocampus (I). The percentage of GFAP-positive area in the DG (D–F) and in the CA1 (H) shows that astroglial cells are less affected by treatment in the hippocampus. $N = 3–4$ per group. Tukey's multiple comparison test: $*P < 0.05$, $**P < 0.01$ vs. the corresponding Sal group; $\#P < 0.05$, $\#\#P < 0.01$, $\#\#\#P < 0.001$ vs. the corresponding CON group; $+ P < 0.05$ vs. the corresponding VPA400 group. Mean ± SEM.

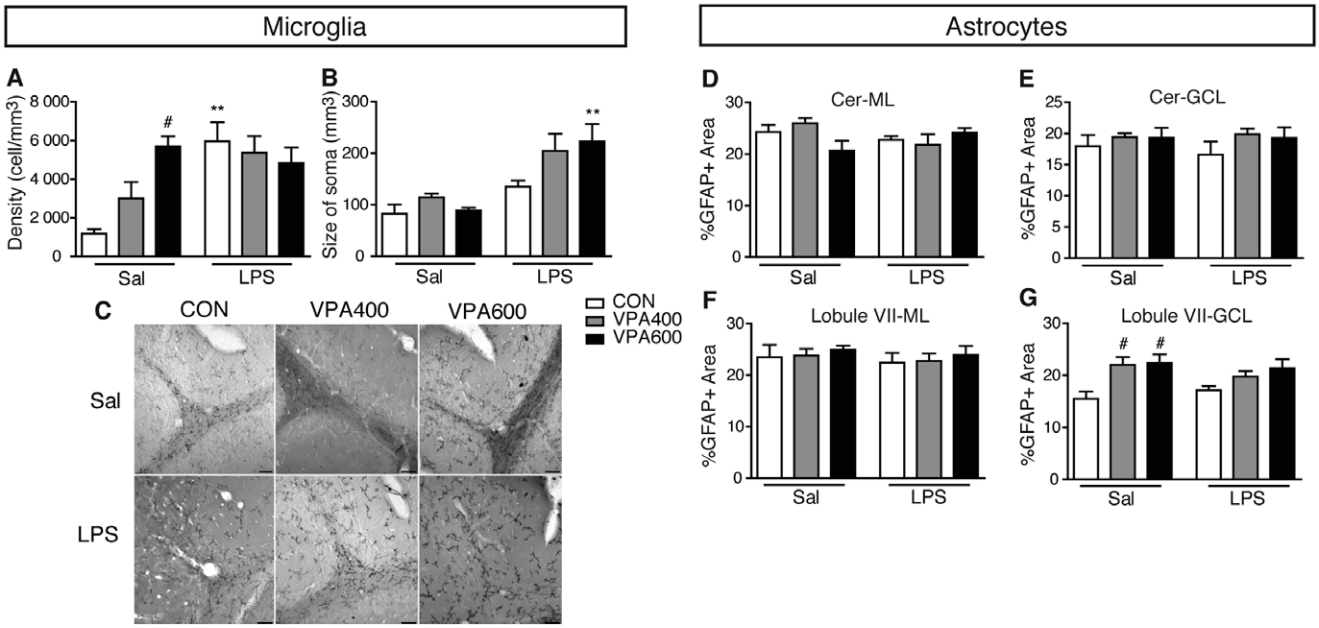

Figure 4. Mice prenatally exposed to valproic acid (VPA) show increased glial activation in the cerebellum. VPA animals have more microglial cells in the cerebellum (A), and these cells show a more activated morphology upon the lipopolysaccharide challenge (B). In (C), we show representative images of immunohistological staining with antibody against CD11b in the lobule VII. Scale bar: 100 μm. No differences on the percentage of GFAP-positive area were observed in the molecular layer (ML, D) or the granular cell layer (GCL, E) of the cerebellum. When the analysis was circumscribed to lobule VII, no differences among groups were observed in the ML (F), but VPA-exposed animals showed an increment on this area (G). $N = 3–4$ per group. Tukey's multiple comparison test: $^{**}P < 0.01$ vs. the corresponding Sal group; $\#P < 0.05$ vs. the corresponding CON group. Mean ± SEM.

lobules of this structure. When we analyzed the area occupied by astrocytes in the different lobules, we observed a significant interaction between treatments in the granular cell layer of lobule VII [$F(2, 17) = 8.747$, $P = 0.002$] due to an increase in this value in animals prenatally exposed to VPA (Fig. 4G and Fig. S3). This effect was not observed in the molecular layer (Fig. 4F), and no differences were observed in the other lobules (data not shown).

Analysis of Cytokine Expression in the Brain of Mice Prenatally Exposed to VPA after a Peripheral Challenge with LPS

To further characterize the glial activation in our model, we analyzed the expression of cytokines in the hippocampus and the cerebellum, both in unchallenged animals and upon the peripheral challenge with LPS. Previous reports have shown that peripheral LPS can induce cytokine expression in the brain [Pitossi et al., 1997]. In all cases, two-way ANOVA (prenatal × adult treatments) followed by Tukey's post-hoc test were performed.

In the hippocampus, IL-1β and IL-6 expression showed an effect of adult treatment [IL-1β, $F(1, 24) = 9.431$, $P = 0.005$; IL-6, $F(1, 24) = 93.954$, $P < 0.001$]. LPS-injected animals showed an increase in the expression of these cytokines, an effect that was more evident for IL-6 (Fig. 5A and B). TNF-α expression showed a different profile, evidencing an interaction between treatments [$F(2, 22) = 13.682$, $P < 0.001$]. CON animals showed a significant increase of hippocampal TNF-α mRNA expression when they were injected with LPS in adulthood, while this effect was blunted in VPA-exposed animals, both in VPA400 and VPA600 mice (Fig. 5C). For the anti-inflammatory cytokine TGF-β1, we found a general effect of prenatal treatment [$F(2, 21) = 4.826$, $P = 0.019$], with VPA600 animals expressing reduced levels of this cytokine regardless of the adult treatment (Fig. 5D).

In the cerebellum, IL-1β expression showed an effect of adult treatment [$F(1, 23) = 7.300$, $P = 0.013$], particularly evident in VPA600 mice (Fig. 5E). Indeed, VPA600-LPS mice showed a tendency to increased IL-1β expression, when compared with VPA600-Sal group ($P = 0.053$). IL-6 and TNF-α expression showed similar profiles in the cerebellum. We observed interactions between prenatal and adult treatments for both cytokines [IL-6, $F(2, 23) = 16.044$, $P < 0.001$; TNF-α, $F(2, 23) = 10.371$, $P < 0.001$]. The increase in cerebellar IL-6 and TNF-α mRNA expression upon LPS challenge was exacerbated in VPA600 mice (Fig. 5F and G). TGF-β1 expression in the cerebellum was not affected by neither prenatal nor adult treatments (Fig. 5H).

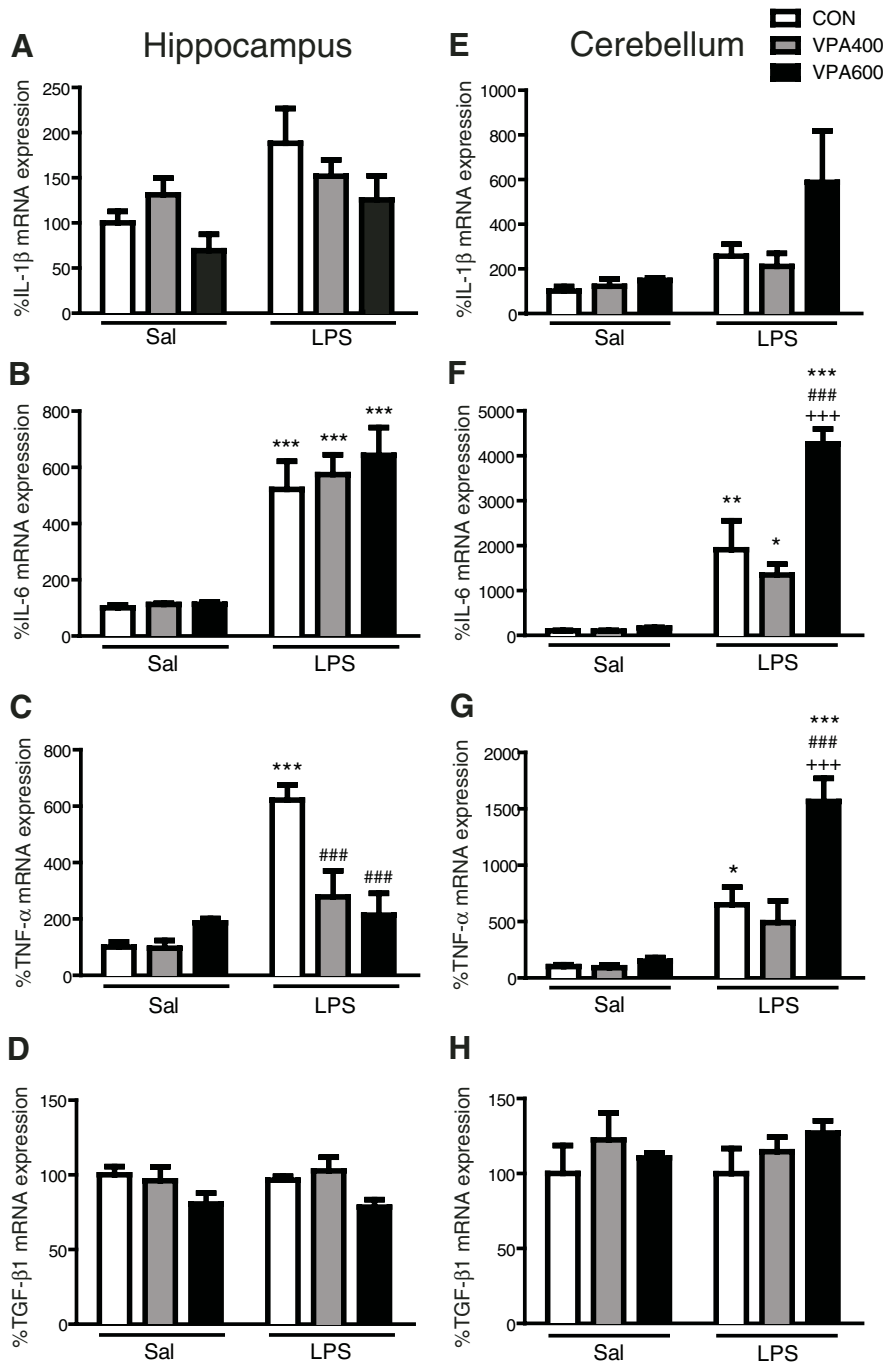

Figure 5. Expression of cytokines in the brains of mice prenatally exposed to valproic acid (VPA): effect of a peripheral lipopolysaccharide (LPS) challenge. IL-1β, IL-6, TNF-α, and TGF-β1 mRNA levels in the hippocampus and cerebellum were determined 2 hr after an LPS challenge. Real-time PCR values are expressed as a percentage of CON-Sal mice. IL-1β expression is not altered in the hippocampus (A), and it showed a tendency to augment in VPA600-LPS group in the cerebellum (E). LPS induces the expression of IL-6 in the hippocampus (B) and in the cerebellum (F), where VPA600 animals show an exacerbated response. Peripheral LPS induces TNF-α expression in both brain regions in CON mice. This increase is prevented in the hippocampus (C) and exacerbated in the cerebellum (G) of VPA600 animals. No differences in the expression of TGF-β1 are observed in the analyzed regions (D and H). $N = 4–6$ per group. Tukey's multiple comparison test: $^{*}P < 0.05$, $^{**}P < 0.01$, $^{***}P < 0.001$ vs. the corresponding Sal group; $^{###}P < 0.001$ vs. the corresponding CON group $P < 0.001$ vs. the corresponding VPA400 group. Mean ± SEM.

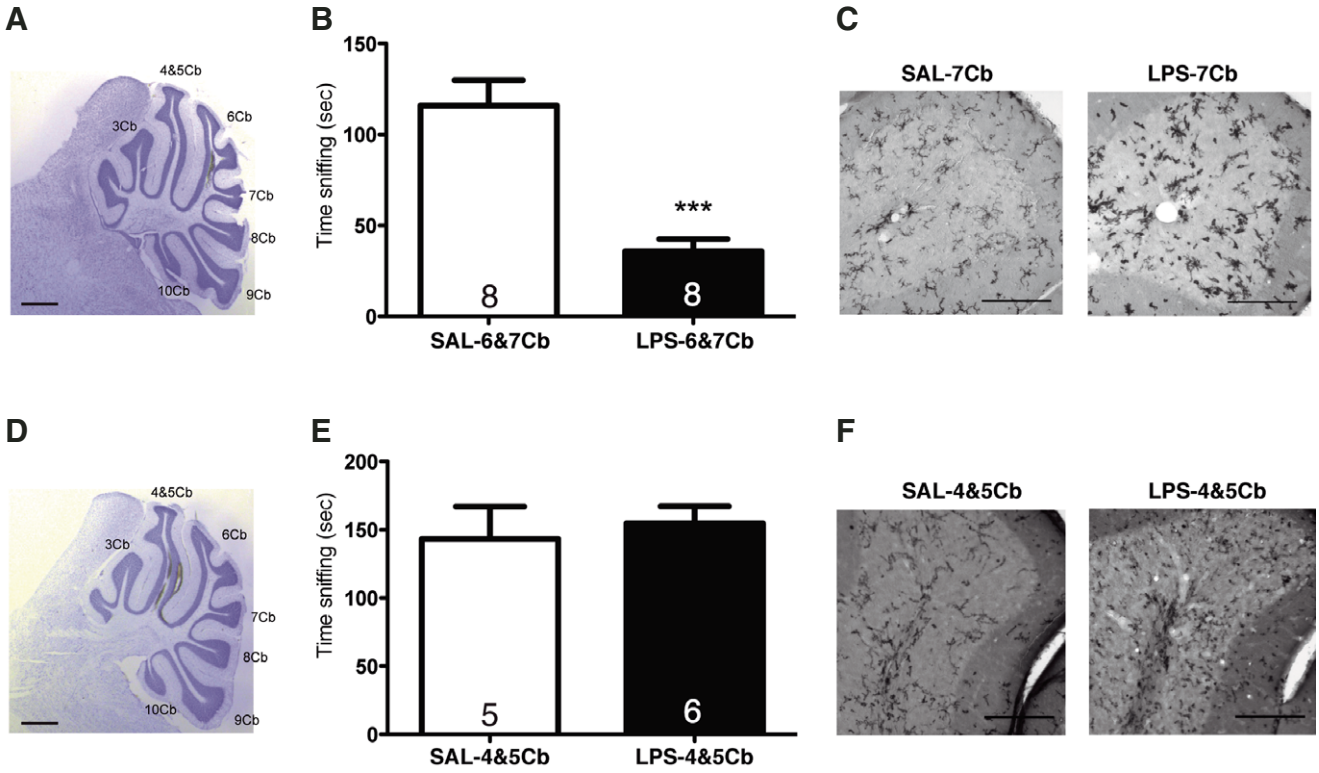

Figure 6. Effect of lipopolysaccharide (LPS) injection into the cerebellum on social interaction. Lobules VI–VII (A) or IV–V (D) were targeted by stereotaxic injections (injections of India ink are shown in Nissl-stained cerebella). The injection of 10 µg LPS into the lobules VI–VII of the cerebellum resulted in reduced social interaction (B) and increased activation of microglial cells in the injected lobules (C, representative photographs of lobule VII with anti-CD11b immunohistochemistry). Stereotaxic injection of 10 µg LPS into the lobules IV–V of the cerebellum did not affect social interaction levels (E), although this treatment resulted in activated microglia in the injected lobules (F, representative photographs of lobule IV–V with anti-CD11b immunohistochemistry). Student's *t*-test: ***$P < 0.001$. Mean ± SEM. Ns are shown in each bar. Cb, cerebellar lobule. Scale bar in A and D, 1 mm; in C and F 150 µm.

Induction of Microglia Activation in the Lobules VI–VII by Intra-Cerebellar LPS Results in Reduced Social Interaction in the Adult Mouse

To evaluate whether the observed neuroinflammation in the adult cerebellum of VPA-exposed mice could underlie the phenotype of reduced social exploration, we stereotaxically injected adult mice with 10 µg of LPS or saline into the lobules VI–VII of the cerebellum (Fig. 6A–C). Twenty-fours after LPS injection, animals showed reduced social interaction (Fig. 6B; $t_{14} = 5.150$, $P < 0.0001$). This effect was not due to a general sickness behavior, as LPS- and saline-injected animals showed similar levels of activity during the test (Sal-6&7Cb, 42.0 ± 3.7 visits, LPS-6&7Cb, 35.0 ± 4.0 visits; $t_{14} = 1.280$, $P = 0.221$) and lost a similar percentage of body weight 24 hr after surgery (Sal-6&7Cb, 5.1 ± 0.8%, LPS-6&7Cb, 6.3 ± 0.7%; $t_{14} = 1.061$, $P = 0.307$).

We then evaluated the neuroinflammatory state of microglia in these animals using the categories described previously [Depino et al., 2011; Kreutzberg, 1996]. Microglia in the lobules VI–VII of LPS-injected mice showed a highly activated morphology (Fig. 6C, right): 38.25 ± 0.12% of the cells presented a macrophage-like morphology (type IV) and 53.75 ± 0.12% of the microglia showed an active (type II/III) morphology ($N = 4$). Conversely, microglial cells present in lobules VI–VII of animals injected with saline (Fig. 6C, left) mainly showed a typically inactive (type I) morphological appearance (99.4 ± 0.01%, $N = 5$).

The effect of cerebellar inflammation on social interaction is specific of lobules VI–VII, as the injection of LPS into lobules IV–V (Fig. 6D–F) did not result in a reduction of sociability 24 hr after (Fig. 6E; $t_9 = 0.664$, $P = 0.664$), although microglia in these lobules was activated upon LPS injection (Fig. 6F).

Discussion

In this work, we show for the first time that mice prenatally exposed to VPA present long-lasting alterations in both peripheral and brain inflammatory responses. Animals prenatally exposed to VPA have normal

corticosterone plasma levels in adulthood. This is in agreement with different clinical studies showing normal cortisol levels in children and adults with ASD [Corbett, Mendoza, Abdullah, Wegelin, & Levine, 2006; Spratt et al., 2012]. However, the normal increase in the concentration of this hormone upon an inflammatory challenge is significantly higher in VPA600 animals than in the CON and VPA400 groups, indicating a hyperreactivity of the HPA axis. Different studies aimed at characterizing the HPA response in children and adults with ASD showed that autistic individuals have increased HPA responses when faced with social and environmental stressors [Corbett et al., 2006; Spratt et al., 2012]. However, these findings do not take into consideration that stressors related to novel experiences and social interactions, which may not be considered as stressful by most individuals, may be especially stressful for those with autism. Accordingly, increased responses could be due to altered perception of stimuli as threatful rather than to an altered HPA function. Here, we chose to evaluate the effect of an immunological stressor to circumvent this possible confounding effect, and verified that indeed the HPA axis function is enhanced in animals prenatally exposed to VPA.

To further characterize the inflammatory response in VPA-exposed animals, we analyzed the expression of proinflammatory cytokines in the spleen, a major lymphoid organ. Ashwood and colleagues showed that higher plasma levels of IL-1β, IL-6, IL-8, and IL-12p40 are associated with highly impaired stereotypical behaviors in ASD [Ashwood et al., 2011], although other studies show normal levels of IL-6 and TNF-α in ASD children [Croonenberghs, Bosmans, Deboutte, Kenis, & Maes, 2002]. In our mouse model, we failed to detect differences in the basal levels of expression of IL-1β, IL-6, or TNF-α. The 25 μg/kg LPS challenge resulted in an increase of IL-1β, IL-6, and TNF-α expression in the spleen 2 hr after the injection, in agreement with a previous report that shows that the expression of these cytokines in the spleen peaks 2 hr after LPS injection [Pitossi et al., 1997]. Interestingly, IL-6 expression after LPS challenge is significantly higher in animals prenatally exposed to VPA than in control mice. Therefore, our results are consistent with previous reports of increased innate immune activity in ASD patients [Jyonouchi et al., 2001]. Moreover, peripheral blood monocytes obtained from ASD children showed increased production of IL-1β, IL-6, and TNF-α when stimulated with the TLR2 ligand LTA, and increased production of IL-1β when stimulated with the TLR4 ligand LPS, when they were compared with the response of cells obtained from age-matched control children [Enstrom, Onore, Van de Water, & Ashwood, 2010]. Whether our mouse model also shows dissimilar patterns of response to particular inflammatory stimuli needs to be further investigated.

Proinflammatory cytokines IL-1β, IL-6, and TNF-α are of special interest in the study of neuroimmunological contributions to psychiatric disorders because they not only act in the periphery but can also increase the neuroinflammatory response and affect brain function. In a first attempt to evaluate the effect of prenatal VPA on glial cells and on the neuroinflammatory response to a peripheral inflammatory challenge, we analyzed the number of microglial cells and the percentage of area occupied by astroglial cells in two brain structures relevant to autism. VPA increased the number of microglial cells in the CA1 of the hippocampus and in the cerebellum. To our knowledge, this is the first report of such a long-term effect of VPA on microglial cells. Different mechanisms could mediate this effect: VPA exposure could alter the proliferation of microglial cells and/or favor the migration of circulating monocytes to the brain parenchyma in these regions during development. Alternatively, VPA treatment could alter glial and/or neuronal function, and neuroinflammation could be elicited in response to this chronic malfunction later in life. Future work will be aimed at determining if this increase in microglia density is observed early in the postnatal brain, or whether it is manifested only later in adulthood.

Our results are in agreement with different postmortem analyses that show microglial activation in different regions of the autistic brain [Morgan et al., 2010; Suzuki et al., 2013; Tetreault et al., 2012; Vargas et al., 2005]. Again, those analyses do not distinguish between early involvement of microglia in ASD and microglial response to other processes taking place in the autistic brain. Our results support the prenatal VPA exposure protocol as a valuable mouse model to evaluate the role and effects of neuroglial alterations on social behavior.

We further tested whether the exacerbated inflammatory response observed in the periphery following LPS injection was also evident in the response of glial cells. In fact, we found that after exposure to LPS, VPA600 mice presented more microglial cells in the molecular layer and the hilus of the DG, and in the CA1 region of the hippocampus than CON mice, lending support to this hypothesis. In the cerebellum, LPS increased the number of microglial cells in CON mice to levels similar to those of the unchallenged VPA600 mice. However, the failure to detect an exacerbated response in VPA600 mice in the cerebellum could be due to a ceiling effect, which precluded us from detecting higher levels of microglial cell activation by measuring proliferation. In line with this, the soma of microglia from the cerebellum of VPA600-LPS mice was larger than that of CON-LPS mice, suggesting their activation. Moreover, in all brain regions and experimental groups, LPS increased the size of microglial cell soma, suggesting activation of these cells. The area occupied by astrocytes, on the other hand, did not show the clear pattern of activation expected for an

exacerbated response to LPS in VPA600 mice. In the cerebellum, astrocytes occupied a larger area in the granular cell layer of lobule VII in both VPA400 and VPA600 mice. Previous work has linked alterations of the normal development of this lobule with reduced sociability in the mouse [DeLorey et al., 2008; Shi et al., 2009], and a reduced size of vermal lobules VI and VII has been found in autistic individuals [Courchesne, Yeung-Courchesne, Press, Hesselink, & Jernigan, 1988].

In addition, we analyzed the expression of proinflammatory cytokines IL-1β, IL-6, and TNF-α, and the anti-inflammatory cytokine TGF-β1, in the same brain structures where glial activation was studied. Remarkably, we found different patterns of expression for each cytokine analyzed. IL-1β only showed a tendency to increase in the cerebellum of VPA600 mice exposed to LPS. The inflammatory stimulus augmented the expression of IL-6 in both brain regions in all experimental groups, but the increment was significantly higher in the cerebellum of VPA600 mice. TNF-α expression was induced 2 hr after LPS injection in both brain regions in CON mice. However, the effect on mice prenatally exposed to VPA was region-specific. VPA600 mice showed an exacerbated response in the cerebellum, but a significantly reduced response in the hippocampus. Finally, none of the experimental groups presented changes in the levels of expression of TGF-β1. We have previously shown a differential effect of TGF-β1 on autism-related behaviors depending on whether it was overexpressed in the young or the adult hippocampus [Depino et al., 2011]. Future work should address whether the expression of this cytokine (along with others) is altered in the postnatal brain in the VPA model, and whether an early neuroinflammatory state also contributes to the behavioral alterations observed in the VPA mouse model of autism.

The different cytokine expression patterns observed after a peripheral LPS stimulus in the brain could be accounted for in part by the fact that we analyzed a single time point after injection. A previous study has shown that IL-1β, IL-6, and TNF-α mRNA levels have different patterns of expression in different brain regions [Pitossi et al., 1997]. Despite this, we clearly observe an exacerbated cytokine expression response in the cerebellum, a region that also shows signs of neuroinflammation at the cellular level. On the contrary, VPA600 mice have more microglial cells and a larger GFAP-positive area in the hippocampus, but the pattern of expression of cytokines in this region does not support an exacerbated response. Further studies will help elucidate the functional consequences of this disparity in the neuroinflammatory state of animals exposed to VPA, and whether there are further consequences when these animals are exposed to stressful stimuli, such as a peripheral inflammogen later in life. This is particularly relevant due to the increased incidence of infection and autoimmune diseases in ASD, which could have an impact on glial function with ensuing consequences on behavior.

As a first attempt to evaluate whether microglial activation in the adult brain can modulate social interaction, we induced microgliosis by stereotaxically injecting LPS into lobules VI–VII of the cerebellum. This central inflammatory stimulus results in reduced sociability 24 hr after the injection and leads microglial cells to a more activated state. Interestingly, sociability is not affected when the LPS is injected in lobules IV–V, stressing the role of cerebellar lobules VI–VII on sociability [Courchesne et al., 1988; DeLorey et al., 2008; Shi et al., 2009]. Future work blocking microglia activation in the brain of VPA mice could help elucidate whether the effect of prenatal VPA on sociability occurs through microglial activation in specific brain regions.

As the behavioral alterations of the VPA model have been previously characterized in various mice and rat strains, our study was mainly focused on repeating those results in an F1 hybrid (C57 x Balb) offspring, a valuable tool to study gene–environment interactions using genetically modified mice [e.g. Carola, Frazzetto, & Gross, 2006]. Our results add to previous work in diverse mouse and rat strains, showing that the reduction in social interaction after prenatal exposure to VPA is a robust response that does not depend on animal genetic background. Similarly, the neuroinflammatory alterations observed in this work need to be verified in other strains to assess the influence of genetic background on this effect of VPA. In particular, our experimental design consists of Balb/c dams and F1 hybrid offspring, and the contribution of these genetic backgrounds to the VPA and inflammatory responses will need to be evaluated by future work.

We measured anxiety- and depression-related behaviors in the F1 hybrid offspring, as mood disorders have a high comorbidity with ASD [American Psychiatric Association, 2000; Hofvander et al., 2009]. To our knowledge, behavioral despair has not been previously analyzed in the VPA model of autism. We found no differences between VPA and CON mice in the tail suspension or forced swimming tests. Although tail suspension and forced swimming tests are not depression models themselves, they are the most reliable tests for assessing antidepressant and/or depression-like behaviors in genetically modified or pharmacologically treated mice [Cryan & Mombereau, 2004]. These results are inconsistent with the high incidence of depression previously reported in individuals with ASD [reviewed in Lainhart, 1999]. Although it has been argued that depression can be difficult to assess in ASD individuals, most studies agree that autistic patients usually present symptoms of depression and respond to antidepressant treatments [Stewart, Barnard, Pearson, Hasan, & O'Brien, 2006]. The lack of depression-related behavior shows

then that the VPA model fails to reproduce this feature of ASD. However, we cannot rule out that the previous behavioral tests could affect the results obtained when evaluating depression-related behavior, as tail suspension and forced swimming tests were the last two tests performed. Moreover, further research could reveal other depression-related behaviors of VPA mice. For example, it would be relevant to evaluate whether VPA-exposed mice are more prone than control mice to develop learned helplessness or depression-like behavior after chronic mild stress, showing then a susceptibility to depression.

The analysis of anxiety-related behavior showed that VPA600 mice explored the open arms of the EPM less than control mice, in agreement with previous reports in CD1 mice [Kataoka et al., 2013] and Wistar rats [Schneider et al., 2008]. However, CD1 mice [Kataoka et al., 2012] did not show the reduction in exploration in the EPM that we observed in the F1 hybrid offspring. In the OF, VPA600 mice showed reduced exploration but no classical anxiety-related behavior (i.e. reduction in the time spent in the center or entries to the center), a behavior that was observed in CD1 mice exposed to VPA [Kataoka et al., 2012]. Although we cannot rule out technical differences that could underlie these discrepancies between the strains [e.g. time between tests was only 1 day in the experiments reported by Kataoka et al., 2012], unpublished data from our group support an alternative interpretation of these results: that the effect of VPA on anxiety-related behaviors is dependent on the genetic background of the animals. Further work is required to test this hypothesis.

All 57 children in the study by Moore and colleagues [Moore et al., 2000] were exposed to VPA during the first trimester of pregnancy, and 51 of them were exposed to anticonvulsants throughout prenatal development. The fact that a single dose of VPA at GD12.5—and not at other gestational ages [Kim et al., 2011]—results in a reduction in sociability in rodents suggests that VPA acts during a critical time window, altering the normal development of the brain circuits regulating this behavior. We hypothesize that there could be a similar critical time window in human development where VPA sensitivity is high, comprised within the chronic exposure period reported by Moore and colleagues.

How an acute exposure to VPA can have long-term consequences on behavior, HPA function, and neuroinflammation still needs to be elucidated. Even though prenatal inflammation can affect both social behavior and immune function in the adult offspring [Hsiao et al., 2012], we showed here that 600 mg/kg VPA does not elicit an inflammatory response in mice, suggesting that VPA acts by at least a partially different mechanism than maternal immune activation. A previous work shows that the effect of prenatal VPA exposure on social behavior is related to its function as a broad-spectrum inhibitor of histone deacetylases [Kataoka et al., 2012]. Moreover, the same study shows a transient hyperacetylated state of histones 3 and 4 in the brain of VPA-exposed pups. In line with this evidence, we hypothesize that this increase in the levels of acetylation can alter gene expression in the brain, and in turn would alter brain development. So, behavioral alterations and/or neuroinflammation could result from this epigenetic effect of VPA. Future work on epigenetic alterations in animals prenatally exposed to VPA will test this hypothesis.

In summary, our results show that the reduction in social interaction observed in a non-inflammatory mouse model of autism (the VPA model) is accompanied by signs of chronic neuroinflammation and to exacerbated peripheral and central responses to a peripheral inflammatory stimulus. This adds to previous evidence of autism-related behavior and immune alterations in a maternal immune activation mouse model of autism [Hsiao et al., 2012; Malkova et al., 2012]. Moreover, these findings contribute to the face validity of the VPA model, recapitulating the neuroinflammatory and immune alterations observed in ASD individuals. Further work using this model will help elucidate the role of inflammatory factors on the development and expression of autism-related behaviors. An improved understanding of neurobiological factors associated with autism may lead to more effective therapeutic interventions, especially in those individuals that reach adulthood and are continuously exposed to infection.

Acknowledgments

This work was supported by a CONICET Grant PIP2010-2012, a University of Buenos Aires Grant UBACyT GEF2010-2012, and an ANPCyT Grant PICT2010-1334. A.M.D. is a member of the Research Career of the National Council of Scientific and Technological Research (CONICET), Argentina. L.L. is fellow of the CONICET. We would like to thank Dr. Fernando Pitossi for his support at the beginning of this project and the access to the StereoInvestigation equipment, and Dr. Lucia Chemes for critical reading of the manuscript.

References

American Psychiatric Association. (2000). Diagnostic and statistical manual of mental disorders, text revision, (4th ed.). Washington, DC: American Psychiatric Association.

Ashwood, P., Krakowiak, P., Hertz-Picciotto, I., Hansen, R., Pessah, I., & Van de Water, J. (2011). Elevated plasma cytokines in autism spectrum disorders provide evidence of immune dysfunction and are associated with impaired behavioral outcome. Brain, Behavior, and Immunity, 25, 40–45.

Banbury Conference. (1997). Mutant mice and neuroscience: Recommendations concerning genetic background. Banbury conference on genetic background in mice. Neuron, 19, 755–759.

Carola, V., Frazzetto, G., & Gross, C. (2006). Identifying interactions between genes and early environment in the mouse. Genes, Brain, and Behavior, 5, 189–199.

Centers for Disease Control and Prevention. (2009). Prevalence of autism spectrum disorders—Autism and developmental disabilities monitoring network, United States, 2006, surveillance summaries, MMWR.

Corbett, B.A., Mendoza, S., Abdullah, M., Wegelin, J.A., & Levine, S. (2006). Cortisol circadian rhythms and response to stress in children with autism. Psychoneuroendocrinology, 31, 59–68.

Courchesne, E., Yeung-Courchesne, R., Press, G.A., Hesselink, J.R., & Jernigan, T.L. (1988). Hypoplasia of cerebellar vermal lobules VI and VII in autism. The New England Journal of Medicine, 318, 1349–1354.

Croonenberghs, J., Bosmans, E., Deboutte, D., Kenis, G., & Maes, M. (2002). Activation of the inflammatory response system in autism. Neuropsychobiology, 45, 1–6.

Cryan, J.F., & Mombereau, C. (2004). In search of a depressed mouse: Utility of models for studying depression-related behavior in genetically modified mice. Molecular Psychiatry, 9, 326–357.

DeLorey, T.M., Sahbaie, P., Hashemi, E., Homanics, G.E., & Clark, J.D. (2008). Gabrb3 gene deficient mice exhibit impaired social and exploratory behaviors, deficits in non-selective attention and hypoplasia of cerebellar vermal lobules: A potential model of autism spectrum disorder. Behavioural Brain Research, 187, 207–220.

Depino, A., Ferrari, C., Pott Godoy, M.C., Tarelli, R., & Pitossi, F.J. (2005). Differential effects of interleukin-1beta on neurotoxicity, cytokine induction and glial reaction in specific brain regions. Journal of Neuroimmunology, 168, 96–110.

Depino, A.M. (2013). Peripheral and central inflammation in autism spectrum disorders. Molecular and Cellular Neurosciences, 53, 69–76.

Depino, A.M., Lucchina, L., & Pitossi, F. (2011). Early and adult hippocampal TGF-beta1 overexpression have opposite effects on behavior. Brain, Behavior, and Immunity, 25, 1582–1591.

Depino, A.M., Tsetsenis, T., & Gross, C. (2008). GABA homeostasis contributes to the developmental programmin g of anxiety-related behavior. Brain Research, 1210, 189–199.

Enstrom, A.M., Onore, C.E., Van de Water, J.A., & Ashwood, P. (2010). Differential monocyte responses to TLR ligands in children with autism spectrum disorders. Brain, Behavior, and Immunity, 24, 64–71.

Garbett, K., Ebert, P.J., Mitchell, A., Lintas, C., Manzi, B., et al. (2008). Immune transcriptome alterations in the temporal cortex of subjects with autism. Neurobiology of Disease, 30, 303–311.

Hofvander, B., Delorme, R., Chaste, P., Nyden, A., Wentz, E., et al. (2009). Psychiatric and psychosocial problems in adults with normal-intelligence autism spectrum disorders. BMC Psychiatry, 9: 35. doi: 10.1186/1471-244X-9-35

Hornig, M., Briese, T., Buie, T., Bauman, M.L., Lauwers, G., et al. (2008). Lack of association between measles virus vaccine and autism with enteropathy: A case-control study. PLoS ONE, 3, e3140. doi:10.1371/journal.pone.0003140

Howard, C.V., & Reed, M.G. (2005). Unbiased stereology. New York: Garland Science/BIOS Scientific.

Hsiao, E.Y., McBride, S.W., Chow, J., Mazmanian, S.K., & Patterson, P.H. (2012). Modeling an autism risk factor in mice leads to permanent immune dysregulation. Proceedings of the National Academy of Sciences of the United States of America, 109, 12776–12781.

Jyonouchi, H., Sun, S., & Le, H. (2001). Proinflammatory and regulatory cytokine production associated with innate and adaptive immune responses in children with autism spectrum disorders and developmental regression. Journal of Neuroimmunology, 120, 170–179.

Kataoka, S., Takuma, K., Hara, Y., Maeda, Y., Ago, Y., & Matsuda, T. (2013). Autism-like behaviours with transient histone hyperacetylation in mice treated prenatally with valproic acid. The International Journal of Neuropsychopharmacology, 16, 91–103.

Kim, K.C., Kim, P., Go, H.S., Choi, C.S., Yang, S.I., et al. (2011). The critical period of valproate exposure to induce autistic symptoms in Sprague-Dawley rats. Toxicology Letters, 201, 137–142.

Kreutzberg, G.W. (1996). Microglia: A sensor for pathological events in the CNS. Trends in Neurosciences, 19, 312–318.

Lainhart, J. (1999). Psychiatric problems in individuals with autism, their parents and siblings. International Review of Psychiatry, 11, 278–298.

Lucchina, L., Carola, V., Pitossi, F., & Depino, A.M. (2010). Evaluating the interaction between early postnatal inflammation and maternal care in the programming of adult anxiety and depression-related behaviors. Behavioural Brain Research, 213, 56–65.

Malik, M., Sheikh, A.M., Wen, G., Spivack, W., Brown, W.T., & Li, X. (2011). Expression of inflammatory cytokines, Bcl2 and cathepsin D are altered in lymphoblasts of autistic subjects. Immunobiology, 216, 80–85.

Malkova, N.V., Yu, C.Z., Hsiao, E.Y., Moore, M.J., & Patterson, P.H. (2012). Maternal immune activation yields offspring displaying mouse versions of the three core symptoms of autism. Brain, Behavior, and Immunity, 26, 607–616.

Martin, L.A., Goldowitz, D., & Mittleman, G. (2010). Repetitive behavior and increased activity in mice with Purkinje cell loss: A model for understanding the role of cerebellar pathology in autism. The European Journal of Neuroscience, 31, 544–555.

McCusker, R.H., & Kelley, K.W. (2013). Immune-neural connections: How the immune system's response to infectious agents influences behavior. The Journal of Experimental Biology, 216, 84–98.

Moore, S.J., Turnpenny, P., Quinn, A., Glover, S., Lloyd, D.J., et al. (2000). A clinical study of 57 children with fetal anticonvulsant syndromes. Journal of Medical Genetics, 37, 489–497.

Morgan, J.T., Chana, G., Pardo, C.A., Achim, C., Semendeferi, K., et al. (2010). Microglial activation and increased microglial density observed in the dorsolateral prefrontal cortex in autism. Biological Psychiatry, 68, 368–376.

Onore, C., Careaga, M., & Ashwood, P. (2012). The role of immune dysfunction in the pathophysiology of autism. Brain, Behavior, and Immunity, 26, 383–392.
Parracho, H.M., Bingham, M.O., Gibson, G.R., & McCartney, A.L. (2005). Differences between the gut microflora of children with autistic spectrum disorders and that of healthy children. Journal of Medical Microbiology, 54, 987–991.
Patterson, P.H. (2011). Maternal infection and immune involvement in autism. Trends in Molecular Medicine, 17, 389–394.
Paxinos, G., & Franklin, K. (2001). The mouse brain in stereotaxic coordinates (2nd ed.). San Diego: Academic Press.
Pitossi, F., del Rey, A., Kabiersch, A., & Besedovsky, H. (1997). Induction of cytokine transcripts in the central nervous system and pituitary following peripheral administration of endotoxin to mice. Journal of Neuroscience Research, 48, 287–298.
Rasband, W.S. (1997–2009). ImageJ. National Institutes of Health, Bethesda, Maryland, USA, http://imagej.nih.gov/ij/.
Rutter, M. (2005). Incidence of autism spectrum disorders: Changes over time and their meaning. Acta Paediatrica, 94, 2–15.
Schneider, T., & Przewlocki, R. (2005). Behavioral alterations in rats prenatally exposed to valproic acid: Animal model of autism. Neuropsychopharmacology, 30, 80–89.
Schneider, T., Roman, A., Basta-Kaim, A., Kubera, M., Budziszewska, B., et al. (2008). Gender-specific behavioral and immunological alterations in an animal model of autism induced by prenatal exposure to valproic acid. Psychoneuroendocrinology, 33, 728–740.
Shanks, N., Windle, R.J., Perks, P.A., Harbuz, M.S., Jessop, D.S., et al. (2000). Early-life exposure to endotoxin alters hypothalamic-pituitary-adrenal function and predisposition to inflammation. Proceedings of the National Academy of Sciences of the United States of America, 97, 5645–5650.
Shi, L., Smith, S.E., Malkova, N., Tse, D., Su, Y., & Patterson, P.H. (2009). Activation of the maternal immune system alters cerebellar development in the offspring. Brain, Behavior, and Immunity, 23, 116–123.
Spratt, E.G., Nicholas, J.S., Brady, K.T., Carpenter, L.A., Hatcher, C.R., et al. (2012). Enhanced cortisol response to stress in children in autism. Journal of Autism and Developmental Disorders, 42, 75–81.
Stewart, M.E., Barnard, L., Pearson, J., Hasan, R., & O'Brien, G. (2006). Presentation of depression in autism and Asperger syndrome: A review. Autism, 10, 103–116.
Suzuki, K., Sugihara, G., Ouchi, Y., Nakamura, K., Futatsubashi, M., et al. (2013). Microglial activation in young adults with autism spectrum disorder. JAMA Psychiatry, 70, 49–58.
Tetreault, N.A., Hakeem, A.Y., Jiang, S., Williams, B.A., Allman, E., et al. (2012). Microglia in the cerebral cortex in autism. Journal of Autism and Developmental Disorders, 42, 2569–2584.
Vargas, D.L., Nascimbene, C., Krishnan, C., Zimmerman, A.W., & Pardo, C.A. (2005). Neuroglial activation and neuroinflammation in the brain of patients with autism. Annals of Neurology, 57, 67–81.
Wagner, G.C., Reuhl, K.R., Cheh, M., McRae, P., & Halladay, A.K. (2006). A new neurobehavioral model of autism in mice: Pre- and postnatal exposure to sodium valproate. Journal of Autism and Developmental Disorders, 36, 779–793.
Wang, L.W., Tancredi, D.J., & Thomas, D.W. (2011). The prevalence of gastrointestinal problems in children across the United States with autism spectrum disorders from families with multiple affected members. Journal of Developmental and Behavioral Pediatrics, 32, 351–360.
West, M.J., Slomianka, L., & Gundersen, H.J. (1991). Unbiased stereological estimation of the total number of neurons in thesubdivisions of the rat hippocampus using the optical fractionator. The Anatomical Record, 231, 482–497.
Yirmiya, R., & Goshen, I. (2011). Immune modulation of learning, memory, neural plasticity and neurogenesis. Brain, Behavior, and Immunity, 25, 181–213.

Supporting Information

Additional Supporting Information may be found in the online version of this article at the publisher's web-site:

Figure S1. Mice prenatally exposed to VPA show increased microglial activation in the molecular layer of the dentate gyrus of the hippocampus after LPS challenge. Representative images of immunohistological staining with antibody against CD11b in the molecular layer of the dentate gyrus (A, DG-ML) and in the granular cell layer of the dentate gyrus (B, DG-GCL). Scale bar: 20 μm.

Figure S2. Mice prenatally exposed to VPA show increased microglial activation in the hilus of the dentate gyrus and in CA1 of the hippocampus after LPS challenge. Representative images of immunohistological staining with antibody against CD11b in the hilus of the dentate gyrus (A, DG-hilus) and in the CA1 of the hippocampus (B, CA1). Scale bar: 20 μm.

Figure S3. Astroglial cells in the hippocampus are less affected by VPA and LPS treatments. Representative images of immunohistological staining with antibody against GFAP in the dentate gyrus (A) and in the CA1 (B). Scale bar: 50 μm.

Figure S4. Mice prenatally exposed to VPA show increased astroglial density in the lobule VII of the cerebellum. Representative images of immunohistological staining with antibody against GFAP in the lobule VII of the cerebellum. Scale bar: 100 μm.